

Aggregated Momentum: Stability Through Passive Damping

James Lucas^{1,2} Richard Zemel^{1,2} Roger Grosse^{1,2}

Abstract

Momentum is a simple and widely used trick which allows gradient-based optimizers to pick up speed in low curvature directions. Its performance depends crucially on a damping coefficient β . Large β values can potentially deliver much larger speedups, but are prone to oscillations and instability; hence one typically resorts to small values such as 0.5 or 0.9. We propose *Aggregated Momentum* (*AggMo*), a variant of momentum which combines multiple velocity vectors with different β parameters. *AggMo* is trivial to implement, but significantly dampens oscillations, enabling it to remain stable even for aggressive β values such as 0.999. We reinterpret Nesterov’s accelerated gradient descent as a special case of *AggMo* and provide theoretical convergence bounds for online convex optimization. Empirically, we find that *AggMo* is a suitable drop-in replacement for other momentum methods, and frequently delivers faster convergence.

1. Introduction

In spite of a wide range of modern optimization research, gradient descent with momentum and its variants remain the tool of choice in machine learning. Momentum methods can help the optimizer pick up speed in low curvature directions without becoming unstable in high-curvature directions. The simplest of these methods, classical momentum (Polyak, 1964), has an associated damping coefficient, $0 \leq \beta < 1$, which controls how quickly the momentum vector decays. There is a fundamental tradeoff between speed and stability: larger β values allow more buildup of velocity, but are more prone to oscillations and instability. In directions where the gradient is small but consistent, the terminal velocity is proportional to $1/(1 - \beta)$, suggesting that β slightly less than 1 could deliver much improved optimization performance. However, large β values are prone to oscillations and instability (O’donoghue & Candes, 2015; Goh, 2017), requiring a smaller learning rate and hence slower convergence.

Other momentum methods have been proposed. Sutskever

¹University of Toronto, Toronto, Ontario, Canada ²Vector Institute, Toronto, Ontario, Canada. Correspondence to: James Lucas <jlucas@cs.toronto.edu>.

et al. (2013) recommended using Nesterov accelerated gradient descent (Nesterov, 1983), which they reinterpreted as a momentum-based method. They found that it was more stable than classical momentum for large β values and gave substantial speedups for training neural networks. However, the reasons for the improved performance remain somewhat mysterious. O’donoghue & Candes (2015) proposed to detect oscillations and eliminate them by resetting the velocity vector to zero. But in practice it is difficult to determine an appropriate restart condition.

In this work, we introduce *Aggregated Momentum* (*AggMo*), a variant of classical momentum which maintains several velocity vectors with different β parameters. *AggMo* adds together the velocity vectors when updating the parameters. We find that this combines the advantages of both small and large β values: the large values allow significant buildup of velocity along low curvature directions, while the small values dampen the oscillations, hence stabilizing the algorithm. *AggMo* is trivial to implement and incurs almost no computational overhead.

We draw inspiration from physics literature when we refer to our method as a form of *passive damping*. Resonance occurs when a system is driven at specific frequencies but may be prevented through careful design (Goldstein, 2011). Passive damping can address this in structures by making use of different materials with unique resonant frequencies. This prevents any single frequency from producing catastrophic resonance. By combining several momentum velocities together we achieve a similar effect — no single frequency is driving the system and so oscillation is prevented.

In this paper we present a theoretical convergence analysis showing that *AggMo* is asymptotically comparable to the best known bound in online convex programming (Zinkevich, 2003). To evaluate *AggMo* empirically we compare against other commonly used optimizers on a range of deep learning architectures: deep autoencoders, convolutional networks, and long-term short-term memory (LSTM).

In all of these cases, we find that *AggMo* works as a drop-in replacement for classical momentum, in the sense that it works at least as well for a given β parameter. But due to its stability at higher β values, it often delivers substantially faster convergence than both classical and Nesterov momentum when its maximum β value is tuned.

2. Momentum-Based Optimization

In this section we briefly review gradient descent with momentum and introduce notation used throughout the rest of this document.

To better understand some of the instability issues present in classical momentum we study its convergence on simple 1-D quadratic functions. We can treat the optimization of quadratic functions as a good approximation for behavior near a local minima. Moreover, for rotation-invariant optimization algorithms we can assume without loss of generality that the quadratic is axis-aligned (Sutskever et al., 2013). Each of the algorithms we study in this section are rotation-invariant. Hence, by restricting to a single dimensional quadratic we are able to reason about the performance of these methods in more general settings.

We exclude adaptive gradient methods, e.g., Adam (Kingma & Ba, 2014), from this analysis. These are not rotation-invariant and in the case of Adam would act as second-order optimizers in this setting.

Classical Momentum We consider a function $f : \mathbb{R}^d \rightarrow \mathbb{R}$ to be minimized with respect to some variable θ . Classical momentum (CM) minimizes this function by taking some initial point θ_0 and running the following iterative scheme,

$$\begin{aligned} \mathbf{v}_t &= \beta \mathbf{v}_{t-1} - \nabla_{\theta} f(\theta_{t-1}) \\ \theta_t &= \theta_{t-1} + \gamma_t \mathbf{v}_t \end{aligned} \quad (1)$$

where γ_t denotes a learning rate schedule, β denotes the damping coefficient and we set $\mathbf{v}_0 = 0$. Although adding momentum can speed up convergence it is often difficult to choose the right damping coefficient, β . Even with momentum, progress in a low curvature direction may be very slow. If the damping coefficient is increased to overcome this then high curvature directions may cause instability and oscillations.

The top row of Figure 1 highlights the failure of CM to adapt to varying curvatures. We aim to optimize 1-D quadratic functions of the form $f(x) = hx^2$. In the left plot we use a low damping coefficient ($\beta = 0.9$) while the right plot shows a high damping coefficient ($\beta = 0.999$). When using a low damping coefficient it takes many iterations to find the optimal solution. On the other hand, increasing the damping coefficient from 0.9 to 0.999 causes oscillations which prevent convergence. When using CM in practice we seek the critical damping coefficient which allows us to rapidly approach the optimum without becoming unstable (Goh, 2017).

Nesterov Momentum Nesterov’s Accelerated Gradient (Nesterov, 1983; 2013) is a modified version of the gradient descent algorithm with improved convergence and stability.

We may write this algorithm as a momentum-based method (Sutskever et al., 2013),

$$\begin{aligned} \mathbf{v}_t &= \beta \mathbf{v}_{t-1} - \nabla_{\theta} f(\theta_{t-1} + \gamma_{t-1} \beta \mathbf{v}_{t-1}) \\ \theta_t &= \theta_{t-1} + \gamma_t \mathbf{v}_t \end{aligned} \quad (2)$$

Nesterov momentum seeks to solve stability issues by correcting the error made after moving in the direction of the velocity, \mathbf{v} . In fact, it can be shown that for a quadratic function Nesterov momentum adapts to the curvature by effectively rescaling the damping coefficients by the eigenvalues of the quadratic (Sutskever et al., 2013). We can see the effect of applying Nesterov Momentum to the 1-D quadratic problem in Figure 1. Nesterov momentum is able to converge more quickly within high curvature regions than CM but retains oscillations for the quadratics exhibiting lower curvature.

3. Passive Damping Through Aggregated Momentum

Aggregated Momentum We propose Aggregated Momentum (AggMo), a variant of gradient descent which aims to improve stability while providing the convergence benefits of larger damping coefficients. We modify the gradient descent algorithm by including several velocity vectors each with their own damping coefficient. At each optimization step these velocities are updated and then averaged to produce the final velocity used to update the parameters. This updated iterative procedure can be written as follows,

$$\begin{aligned} \mathbf{v}_t^{(i)} &= \beta^{(i)} \mathbf{v}_{t-1}^{(i)} - \nabla_{\theta} f(\theta_{t-1}), \text{ for all } i \\ \theta_t &= \theta_{t-1} + \frac{\gamma_t}{K} \sum_{i=1}^K \mathbf{v}_t^{(i)} \end{aligned} \quad (3)$$

where $\mathbf{v}_0^{(i)} = 0$ for each i . The velocities, $\mathbf{v}_t^{(i)}$, are first updated using their corresponding damping coefficients, $\beta^{(i)}$. These velocities are then averaged to update the parameters θ_t . We refer to the vector $\beta = [\beta^{(1)}, \dots, \beta^{(K)}]$ as the *damping vector*.

By taking advantage of several damping coefficients we are able to passively adapt to regions of varying curvature within our objective function. In regions of low curvature the velocity corresponding to largest damping coefficient $\beta^{(i)}$ will dominate the parameter updates. If the optimization procedure enters a region of high curvature with rapidly changing directions (e.g. oscillations) then the velocities corresponding to smaller $\beta^{(i)}$ values will adapt more quickly reducing the overall magnitude of the updates. Figure 1 shows the optimization of 1-D quadratic objectives with varying curvatures using aggregated momentum. By averaging several velocities we can optimize quickly in both high curvature and low curvature regions.

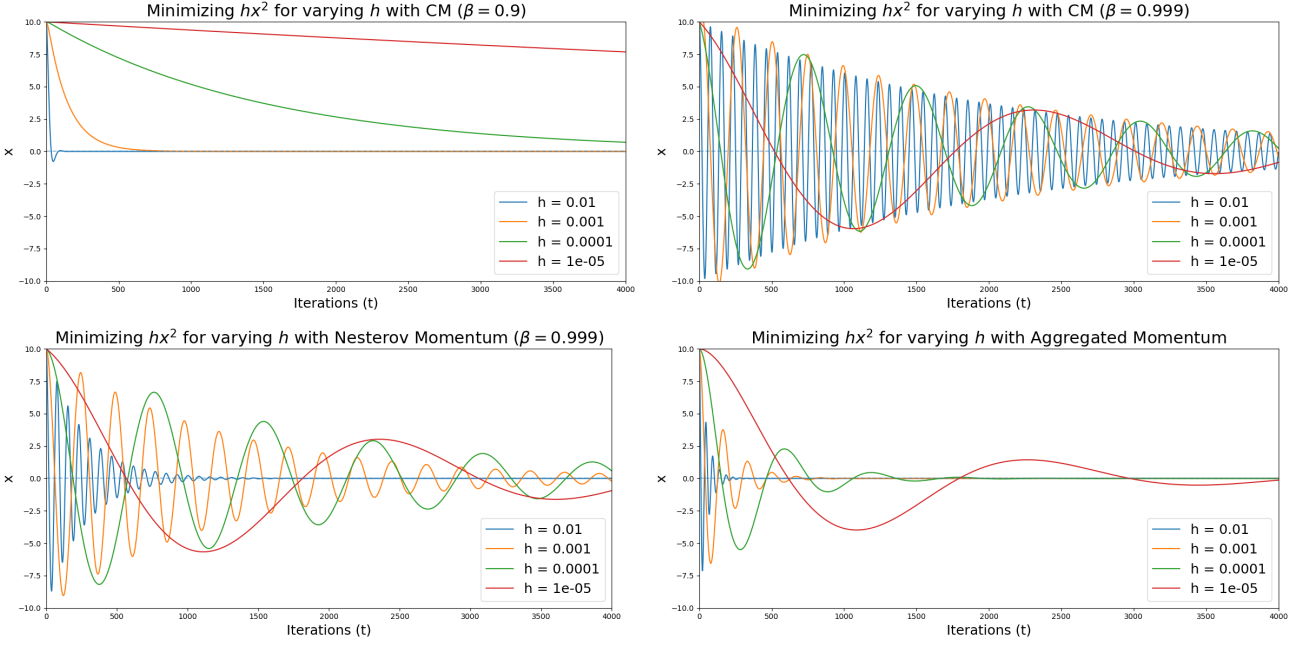


Figure 1. Optimizing quadratics with varying curvatures In this figure we are studying the optimization of functions of the form $f(x) = hx^2$. The top row displays classical momentum with $\beta = 0.9$ (left) and $\beta = 0.999$ (right). The bottom row displays Nesterov momentum (left) with $\beta = 0.999$ and our proposed method, AggMo (right) with $\beta = [0, 0.9, 0.99, 0.999]$.

Choosing the Damping Vector We find in practice that AggMo is robust to choices of the damping vector. In our experiments we found that it is valuable to include a damping coefficient of zero. This increases the weight of the update in the direction of the current gradient. We found that $\beta = [0, 0.9, 0.99]$ is a good default in most tasks. We explore the effect of varying the damping vector in Section 7.1.

Computational/Memory Overhead There is very little additional computational overhead when using AggMo compared to CM. Most optimization problems, especially those that arise in deep learning, will be dominated by the gradient computation and not the velocity aggregation.

AggMo aims to improve on classical momentum by using multiple velocities. The single velocity vector in CM will have the same size as the number of parameters to be optimized. In our method we require K such vectors; meaning if there are many parameters, as in neural networks, this could prove memory-intensive. However, in modern neural network architectures it is typically the activations which dominate the memory cost - not the network parameters (Gomez et al., 2017; Chen et al., 2016). This is especially pronounced in recurrent neural networks (Werbos, 1990; Hochreiter & Schmidhuber, 1997) where the activations may be orders of magnitude larger in memory than the parameters.

4. Recovering Nesterov Momentum

In this section we show that we can approximately recover Nesterov Momentum (Equation 2) as a special case of Aggregated Momentum (Equation 3).

Consider Aggregated Momentum with only two velocities and a constant learning rate, $\gamma_t = 2\gamma$. If we set the damping vector to $\beta = [0, \beta]$, then the update rule from Equation 3 can be written as,

$$\begin{aligned} \mathbf{v}_t &= \beta \mathbf{v}_{t-1} - \nabla_{\theta} f(\boldsymbol{\theta}_{t-1}) \\ \boldsymbol{\theta}_t &= \boldsymbol{\theta}_{t-1} + \gamma \beta \mathbf{v}_{t-1} - 2\gamma \nabla_{\theta} f(\boldsymbol{\theta}_{t-1}) \end{aligned} \quad (4)$$

Similarly, we may write the Nesterov Momentum update with constant learning rate $\gamma_t = \gamma$ as,

$$\begin{aligned} \mathbf{v}_t &= \beta \mathbf{v}_{t-1} - \nabla_{\theta} f(\boldsymbol{\theta}_{t-1} + \gamma \beta \mathbf{v}_{t-1}) \\ \boldsymbol{\theta}_t &= \boldsymbol{\theta}_{t-1} + \gamma \beta \mathbf{v}_{t-1} - \gamma \nabla_{\theta} f(\boldsymbol{\theta}_{t-1} + \gamma \beta \mathbf{v}_{t-1}) \end{aligned} \quad (5)$$

Now we consider Equation 5 when using the reparameterization given by $\boldsymbol{\phi}_t = \boldsymbol{\theta}_t + \gamma \beta \mathbf{v}_t$,

$$\begin{aligned} \boldsymbol{\phi}_t - \gamma \beta \mathbf{v}_t &= \boldsymbol{\phi}_{t-1} - \gamma \nabla_{\theta} f(\boldsymbol{\phi}_{t-1}) \\ \Rightarrow \boldsymbol{\phi}_t &= \boldsymbol{\phi}_{t-1} + \gamma \beta \mathbf{v}_t - \gamma \nabla_{\theta} f(\boldsymbol{\phi}_{t-1}) \\ &= \boldsymbol{\phi}_{t-1} + \gamma \beta^2 \mathbf{v}_{t-1} - (1 + \beta) \gamma \nabla_{\theta} f(\boldsymbol{\phi}_{t-1}) \end{aligned} \quad (6)$$

Thus, under the given reparameterization scheme and in the setting where β is sufficiently close to 1 the Nesterov

momentum update is approximately the same as this special case of aggregated momentum. We demonstrate this approximate equivalence empirically in the appendix.

5. Convergence of AggMo

We evaluate the convergence rate of AggMo in the setting of online convex programming, as proposed in Zinkevich (2003). We consider a sequence of unknown convex cost functions, $f_1(\boldsymbol{\theta}), \dots, f_T(\boldsymbol{\theta})$. At each time t we aim to predict the parameter $\boldsymbol{\theta}_t$ which minimizes the regret,

$$R(T) = \sum_{t=1}^T [f_t(\boldsymbol{\theta}_t) - f_t(\boldsymbol{\theta}^*)] \quad (7)$$

where $\boldsymbol{\theta}^*$ is the fixed point parameter minimizing $\sum_{t=1}^T f_t(\boldsymbol{\theta}^*)$. We are able to show that AggMo has regret bounded by $O(\sqrt{T})$ - a result asymptotically comparable to the best known bound (Duchi et al., 2011). We adopt the following definitions from (Duchi et al., 2011) to simplify the notation. We write $g_t = \nabla f_t(\boldsymbol{\theta}_t)$ with $g_{t,i}$ as the i^{th} element of this vector. Additionally, we write $g_{1:T,i} \in \mathbb{R}^T$ as the vector containing the i^{th} element of the gradient over the first t iterations; $g_{1:T,i} = [g_{1,i}, \dots, g_{t,i}]$. Then the following theorem holds,

Theorem 1. *Assume that f_t has bounded gradients, $\|\nabla f_t(\boldsymbol{\theta})\|_2 < G$, $\|\nabla f_t(\boldsymbol{\theta})\|_\infty < G_\infty$, $\forall \boldsymbol{\theta} \in \mathbb{R}^d$. Moreover, assume that each $\boldsymbol{\theta}_t$ generated by AggMo satisfies $\|\boldsymbol{\theta}_n - \boldsymbol{\theta}_m\|_2 \leq D$, $\|\boldsymbol{\theta}_n - \boldsymbol{\theta}_m\|_\infty \leq D_\infty$ for all $m, n \in \{1, \dots, T\}$. Let $\gamma_t = \frac{\gamma}{\sqrt{t}}$ and $\beta_t^{(i)} = \beta^{(i)} \lambda^t$, $\lambda \in (0, 1)$. Then AggMo achieves the following regret bound, for all $T \geq 1$.*

$$\begin{aligned} R(T) &\leq \frac{KD_\infty^2 \sqrt{T}}{\gamma} \\ &+ \sqrt{1 + \log(T)} \sum_{j=1}^d \|g_{1:T,j}\|_4^2 \sum_{i=1}^K \frac{1 + \beta^{(i)}}{(1 - \beta^{(i)})^2} \\ &+ \frac{D^2}{2\gamma(1 - \lambda)^2} \sum_{i=1}^K \beta^{(i)} \end{aligned}$$

The proof is given in the appendix. Note that this result requires both a decaying learning rate and a decaying damping coefficient, both of which are critical in the analysis. The bounded trajectory assumption will hold in the setting of constrained optimization over a bounded set with each update projected into the viable space.

It immediately follows that the average regret of AggMo converges, i.e. that $R(T)/T \rightarrow 0$. Observing that $\|g_{1:T,j}\|_4^2 \leq G_\infty^2 \sqrt{T}, \forall j$. We also note that this bound may be significantly better than the one obtained for SGD if we have $\sum_{j=1}^d \|g_{1:T,j}\|_4^2 \ll \sqrt{dT}$ (Duchi et al., 2011).

6. Related Work

Sutskever et al. (2013) explored the effect of momentum on the optimization of neural networks and introduce the momentum view of Nesterov's accelerated gradient. They focused on producing good momentum schedules during optimization to adapt to ill-conditioned curvature. Despite strong evidence that this approach works well, practitioners today still typically opt for a fixed momentum schedule and vary the learning rate instead.

Adaptive gradient methods have been introduced to deal with the ill-conditioned curvature we often observe in machine learning (Duchi et al., 2011; Kingma & Ba, 2014; Zeiler, 2012; Tieleman & Hinton, 2012). Kingma & Ba (2014) introduced the Adam optimizer, which utilizes a diagonal approximation to the curvature of the objective function. This technique produces a stable optimization scheme which is easy to use and produces strong results. However, some questions remain on the usability of Adam in more challenging regimes. For example, Wilson et al. (2017) highlight the inability of Adam and other adaptive methods to generalize as well as classical momentum on challenging deep learning tasks. The authors found that while Adam is able to optimize more quickly than classical momentum it often plateaus on the validation set sooner. In this work we also observe Adam's failure to generalize across a range of tasks, but find that AggMo is typically able to improve convergence without sacrificing generalization.

Another line of adaptive methods seeks to detect when oscillations occur during optimization. O'donoghue & Candes (2015) proposed using an adaptive restarting scheme to remove oscillations whenever they are detected. In its simplest form, this is achieved by setting the momentum velocity to zero whenever the loss increases. Further work (Srinivasan et al., 2018) has suggested using an adaptive momentum schedule instead of zeroing. Although this technique works well for well-conditioned convex problems it is difficult to find an appropriate restart condition for the ill-conditioned non-convex problems that we observe in machine learning. On the other hand, AggMo's passive damping approach addresses the oscillation problem without the need to detect its occurrence.

Natural Gradient Descent (Amari, 1998) makes full use of the local curvature during optimization by computing and inverting the full Hessian matrix. Unfortunately, this requires huge computational and memory overhead when the number of parameters to be optimized is large - as in deep neural networks. To overcome these issues, several approximations to natural gradient descent have been proposed (Martens & Grosse, 2015; Martens, 2010). These methods replace the Hessian with a close approximation or avoid computing it entirely. Despite their effectiveness, these methods have not been adopted by the community at large. We believe this is mostly due to their difficulty of implementation and the additional hyperparameters they introduce (e.g. structural

damping).

7. Evaluation

We evaluated the AggMo optimizer on the following three deep learning tasks; Autoencoders, CNN Classification, and LSTM Language Modeling. To do so we used four datasets: MNIST (LeCun et al., 1998), CIFAR-10, CIFAR-100 (Krizhevsky & Hinton, 2009) and Penn Treebank (Marcus et al., 1993).

In each of these tasks we compared AggMo to classical momentum, Nesterov momentum, and Adam. In each experiment we performed a grid search over the learning rate and the damping coefficient/vector while keeping other network hyperparameters fixed. Full details of the experimental set up for each task can be found in the appendix.

For each of the following experiments we choose to report the validation and test performance of the network in addition to the final training loss when it is meaningful to do so. Although this is not typical when presenting an optimization algorithm, recent work has shown that the choice of optimizer may have a significant effect on the generalization error of the network in practice (Wilson et al., 2017). As we are primarily interested in the application of AggMo to machine learning problems we explicitly report on its generalization performance.

7.1. Autoencoders

We trained fully-connected Autoencoders on the MNIST dataset using a set-up similar to that described in Sutskever et al. (2013). The primary difference is the way in which hyperparameters are chosen. Their work focuses on finding an optimal momentum schedule while we keep the momentum fixed but instead apply a simple learning rate decay schedule. For CM, Adam and Aggmo we searched over the following range of learning rates: $\{0.1, 0.05, 0.01, 0.005, 0.001, 0.0005, 0.0001, 0.00005, 0.00001\}$. With CM and Nesterov we evaluated damping coefficients in the range: $\{0.0, 0.9, 0.99, 0.999\}$. For Adam it is standard to use $\beta_1 = 0.9$ and $\beta_2 = 0.999$. We chose to search over $\beta_1 = \{0.9, 0.99, 0.999\}$ and keep $\beta_2 = 0.999$. For the AggMo optimizer we explored damping vectors composed of coefficients that increase logarithmically, beginning with $\beta = [0, 0.9]$ and increasing up to $\beta = [0, 0.9, 0.99, 0.999, 0.9999]$. The models are trained for 1000 epochs using a fixed learning rate schedule: decaying by a factor of 10 after 200, 400 and finally 800 epochs.

We report the training, validation, and test errors in Table 1. Results are displayed for the hyperparameters which achieved the best training loss and also for those that achieved the best validation loss. For Nesterov momentum the same hyperparameters achieved the best training and validation performance. Aggmo achieved the lowest training loss but had a worse validation loss than Nesterov

in this case. Adam optimized to a worse training loss than AggMo but did so with a larger generalization error. When tuning with the validation loss, AggMo achieved the lowest error on both the validation and test sets.

In these experiments the optimal damping coefficient for both CM and Nesterov was $\beta = 0.99$ while the optimal damping vector for AggMo was $\beta = [0.0, 0.9, 0.99, 0.999]$. In Figure 2 we compare the convergence of each of the optimizers. The optimal hyperparameters for the training loss is used in each case. The largest difference in convergence is observed with classical momentum which is considerably slower than the other algorithms. Adam initially converges quickly but plateaus much earlier than Nesterov momentum and AggMo on the validation loss. This matches the observation of Wilson et al. (2017) that adaptive gradient methods such as Adam tend to overfit more aggressively than classical momentum.

Increasing Damping During our experiments we observed that AggMo remains stable during optimization for learning rates an order of magnitude (or more) larger than is possible for CM and Nesterov with β equal to the max damping coefficient used in AggMo. This is evidence for AggMo’s ability to dampen oscillations even with large momentum values.

We further investigated the effect of increasing the maximum damping coefficient of AggMo in Figure 3. The learning rate is fixed at 0.1 and the damping vectors begin at $\beta = [0, 0.9]$ and increase logarithmically up to $\beta = [0, 0.9, 0.99, 0.999, 0.9999]$. We compared to Nesterov with damping coefficients in the same range and a fixed learning rate of 0.05 (to be consistent with our analysis in Section 4). Only the curves that are stable during optimization are displayed.

AggMo was able to remain stable with a maximum damping coefficient of 0.999 whereas Nesterov was stable only at $\beta \in \{0.9, 0.99\}$. While the convergence rates are similar for the range in which Nesterov is stable, AggMo is able to take advantage of the larger damping coefficient of 0.999 and has the fastest overall convergence.

Momentum Finetuning Sutskever et al. (2013) observed that reducing momentum in the last few stages of optimization significantly improved results for momentum based optimization. We investigated this for AggMo by removing the larger damping coefficients from the damping vector towards the end of optimization, leaving $\beta = [0, 0.9]$. We found that when using a learning rate schedule this method has only a small effect on the optimization. This aligns with the discussion in Sutskever et al. (2013) during which the authors refer to the “transient phase” of optimization in which the descent is fast along the error surface. Momentum finetuning is most useful when applied towards the end of the transient phase and before the network begins to overfit.

Optimizer	Train Optimal			Validation Optimal		
	Train Loss	Val. Loss	Test Loss	Train Loss	Val. Loss	Test Loss
CM	2.51 \pm 0.06	5.38 \pm 0.13	5.40 \pm 0.13	2.86 \pm 0.09	3.55 \pm 0.15	3.45 \pm 0.15
Nesterov	1.52 \pm 0.02	3.20 \pm 0.01	3.13 \pm 0.02	1.52 \pm 0.02	3.20 \pm 0.01	3.13 \pm 0.02
Adam	1.44 \pm 0.02	3.97 \pm 0.07	3.91 \pm 0.07	1.48 \pm 0.02	3.80 \pm 0.04	3.72 \pm 0.05
AggMo	1.39 \pm 0.02	3.63 \pm 0.06	3.60 \pm 0.06	2.14 \pm 0.04	3.05 \pm 0.03	2.96 \pm 0.03

Table 1. MNIST Autoencoder MSE across different optimizers. We display the train, validation, and test errors for the optimization run that produced the best training loss and also for the run with the best validation loss. In each case the average loss and standard deviation over 15 runs is displayed.

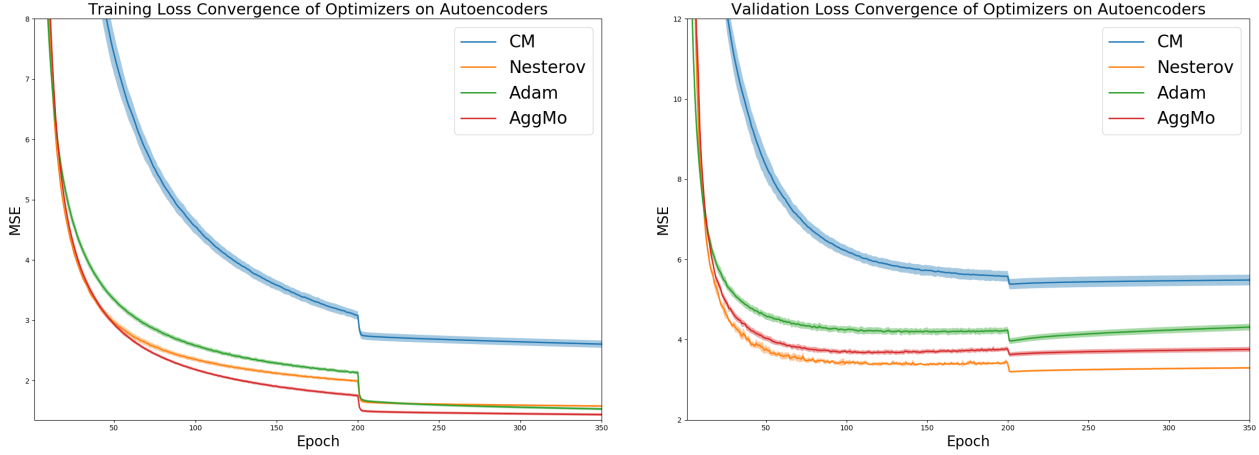


Figure 2. Convergence of Autoencoders Here we show the training and validation loss during the first 350 epochs of training with each optimizer. For each model we use the hyperparameters which obtained the best training loss.

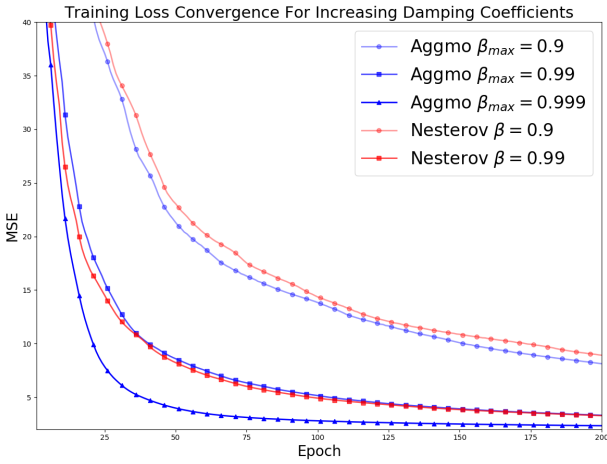


Figure 3. Damping Coefficient Investigation Optimizing autoencoders on MNIST with varying damping coefficients and fixed learning rate. AggMo is in blue and Nesterov in red, with decreasing opacity corresponding to smaller damping coefficients. We do not include the curves for which training is unstable: Nesterov with $\beta \in \{0.999, 0.9999\}$ and AggMo with $\beta_{max} = 0.9999$

We found that if we use a fixed learning rate then momentum finetuning is able to provide a significant improvement for both Nesterov momentum and AggMo.

7.2. Classification

We now shift our focus away from fully-connected networks and instead train convolutional neural networks (CNNs) for image classification. For these experiments we used two different network architectures: a neural network with 5 convolutional layers (CNN-5) and the ResNet-34 architecture (He et al., 2016).

We evaluated CNN-5 on CIFAR-10 only and without any regularization or data augmentation. The ResNet-34 model was trained on both CIFAR-10 and CIFAR-100 with weight decay, batch normalization, and data augmentation (random crops and random horizontal flips). In these experiments we searched over the following learning rates for all optimizers: $\{0.1, 0.05, 0.01, 0.005, 0.001, 0.0005, 0.0001\}$. We searched over the same damping coefficients as in the autoencoder experiments. Each model was trained for a total of 500 epochs.

For each optimizer we report the accuracy on a randomly held out validation set and the test set. The results are displayed in Table 2. For both of the CIFAR-10 experiments we observed the best validation accuracy using the AggMo

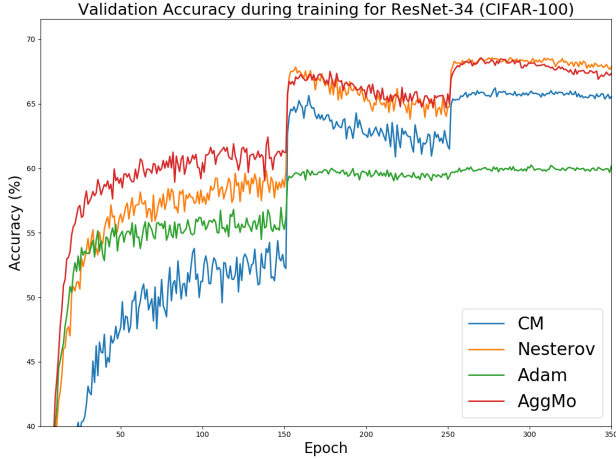


Figure 4. ResNet-34 Trained On CIFAR-100 The validation accuracy during training on CIFAR-100 for each optimizer.

optimizer. However, for both of the ResNet models trained we find that Nesterov momentum is able to achieve a better test set accuracy even with equal or worse validation.

We observed the most significant gap in the generalization performance of Adam and the other optimizers on the CIFAR-100 dataset. Adam was able to effectively reduce the training error but even with early stopping was unable to match the validation performance of the other momentum-based methods.

Figure 4 shows the validation accuracy during training with each of the optimizers used to train the ResNet-34 model. The hyperparameters used for each plot are those which obtained the best validation accuracy. We see that AggMo converges most quickly at first but is met by Nesterov after the first learning rate decay. We observe early flat-lining of Adam as described in Wilson et al. (2017).

We note that the additional network hyperparameters (e.g. weight decay) are defaults which were likely picked as they work well with classical momentum. This may give a disadvantage to the other optimizers, including our own. Despite this, we found that we are able to outperform CM with the AggMo and Nesterov optimizers without additional tuning of any of these hyperparameters.

7.3. Language Modeling

We trained LSTM Language Models on the Penn Treebank dataset. We followed the experimental setup of Merity et al. (2017) and made use of the code provided by the authors. We used the optimal hyperparameter settings described by the authors and vary only the learning rate, momentum and whether gradient clipping is used. We note that these hyperparameters were tuned using SGD and may not be optimal for the other optimizers we evaluate (including our

own). We followed only the base model training used in Merity et al. (2017) and do not include the fine-tuning and continuous cache optimization steps.

For SGD, CM, AggMo and Nesterov we searched over learning rates in the range $\{50, 30, 10, 5, 2.5, 1, 0.1, 0.01\}$. We found that Adam required much smaller learning rates in this setting and so searched over values in the range $\{0.1, 0.05, 0.01, 0.005, 0.001, 0.0005, 0.0001\}$. We searched over the damping coefficients as in the previous experiments. Each model was trained for 750 epochs, as in Merity et al. (2017).

Table 3 contains the results for the hyperparameter settings which achieved the best validation error for each optimizer. The first row (denoted *) uses the ASGD (Polyak & Juditsky, 1992) scheme suggested in Merity et al. (2017): once the validation loss plateaus we switch to the ASGD optimizer. The other rows instead decay the learning rate when the validation loss plateaus.

As noted in Merity et al. (2017), it is typically observed that SGD without momentum performs better than momentum based methods in language modeling tasks. We found that this is true for classical momentum. However, in our experiments we observed that the other momentum-based optimizers outperform both ASGD and SGD without momentum. Surprisingly, we found that Adam is well-suited to this task and achieves the best training, validation, and test performance. We believe that the heavy regularization used when training the network makes Adam a good choice. AggMo is very close in terms of final performance to Adam.

While gradient clipping is critical for SGD without momentum, which utilizes a large learning rate, we found that all of the momentum methods perform better without gradient clipping. This is likely due to the use of lower learning rates.

Figure 5 compares the convergence of the training and validation perplexity of each optimizer. While the momentum based methods converge after 300 epochs, the momentum-free methods converged much more slowly. Surprisingly, we found that SGD worked best without any learning rate decay. Adam converged most quickly and achieved a validation perplexity which is comparable to that of AggMo.

These experiments suggest that there is more to the optimization of these models than is currently understood. While existing work encourages practitioners to avoid momentum we found that using momentum may significantly improve convergence rates and final performance.

8. Conclusion

Aggregated Momentum is a simple extension to classical momentum which is easy to implement and has negligible computational overhead on modern deep learning tasks. We showed empirically that AggMo is able to remain stable

Optimizer	CNN-5 (CIFAR-10)		ResNet-34 (CIFAR-10)		ResNet-34 (CIFAR-100)	
	Val. Acc. (%)	Test Acc. (%)	Val. Acc. (%)	Test Acc. (%)	Val. Acc. (%)	Test Acc. (%)
CM	64.1	63.43	92.38	92.04	66.23	65.68
Nesterov	65.14	64.32	92.85	92.34	68.56	68.68
Adam	63.67	62.86	91.09	90.43	60.25	60.83
AggMo	65.98	65.09	92.87	91.65	68.56	68.16

Table 2. Classification performance on CIFAR-10 and CIFAR-100 We display results using the optimal hyperparameters for CM, Nesterov, Adam and AggMo on the validation set.

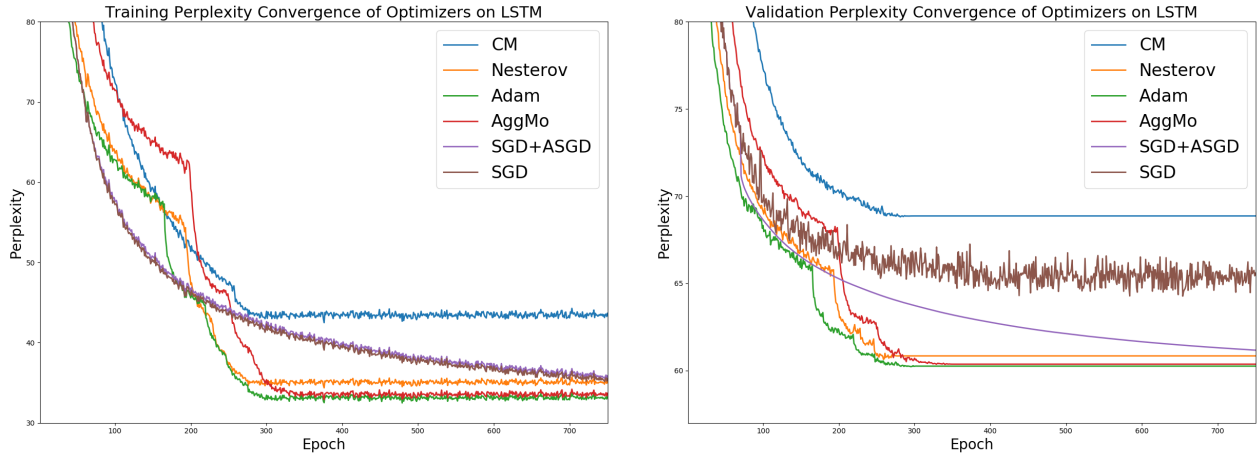


Figure 5. Convergence of LSTM The training and validation perplexity during training. For each model we use the hyperparameters that obtained the best validation loss.

Optimizer	Train Perplexity	Val. Perplexity	Test Perplexity
*SGD + ASGD	35.68	61.17	59.26
SGD	35.34	63.39	62.41
CM	50.34	70.37	68.21
Nesterov	34.91	60.84	58.44
Adam	32.88	60.25	57.83
AggMo	33.22	60.36	57.79

Table 3. Penn Treebank LSTM Perplexity across different optimizers. We display the train, validation, and test error for the optimization run that produced the best validation loss. * uses ASGD (Polyak & Juditsky, 1992) and corresponds to the base model reported in Merity et al. (2017)

even with large damping coefficients and enjoys faster convergence rates as a consequence of this. We found that despite its relative lack of popularity, Nesterov momentum also performed very well. On the tasks we explored, AggMo could be used as a drop-in replacement for existing optimizers with little-to-no additional hyperparameter tuning.

9. Acknowledgements

We would like to thank Geoffrey Hinton for suggesting the link between AggMo and passive damping in physical systems. We also thank Paul Vicol for his help with the LSTM experiments. Finally, we thank our many other colleagues for useful discussions and insights. James Lucas is supported by an NSERC research grant.

References

Amari, Shun-Ichi. Natural gradient works efficiently in learning. *Neural computation*, 10(2):251–276, 1998.

Chen, Tianqi, Xu, Bing, Zhang, Chiyuan, and Guestrin, Carlos. Training deep nets with sublinear memory cost. *arXiv preprint arXiv:1604.06174*, 2016.

Duchi, John, Hazan, Elad, and Singer, Yoram. Adaptive subgradient methods for online learning and stochastic optimization. *Journal of Machine Learning Research*, 12 (Jul):2121–2159, 2011.

Goh, Gabriel. Why momentum really works. *Distill*, 2(4):e6, 2017.

Goldstein, Herbert. *Classical mechanics*. Pearson Education India, 2011.

Gomez, Aidan N, Ren, Mengye, Urtasun, Raquel, and Grosse, Roger B. The reversible residual network: Back-propagation without storing activations. In *Advances in Neural Information Processing Systems*, pp. 2211–2221, 2017.

He, Kaiming, Zhang, Xiangyu, Ren, Shaoqing, and Sun, Jian. Deep residual learning for image recognition. In *Proceedings of the IEEE conference on computer vision and pattern recognition*, pp. 770–778, 2016.

Hochreiter, Sepp and Schmidhuber, Jürgen. Long short-term memory. *Neural computation*, 9(8):1735–1780, 1997.

Kingma, Diederik and Ba, Jimmy. Adam: A method for stochastic optimization. *arXiv preprint arXiv:1412.6980*, 2014.

Krizhevsky, Alex and Hinton, Geoffrey. Learning multiple layers of features from tiny images. 2009.

LeCun, Yann, Bottou, Léon, Bengio, Yoshua, and Haffner, Patrick. Gradient-based learning applied to document recognition. *Proceedings of the IEEE*, 86(11):2278–2324, 1998.

Marcus, Mitchell P, Marcinkiewicz, Mary Ann, and Santorini, Beatrice. Building a large annotated corpus of english: The penn treebank. *Computational linguistics*, 19(2):313–330, 1993.

Martens, James. Deep learning via hessian-free optimization. In *ICML*, volume 27, pp. 735–742, 2010.

Martens, James and Grosse, Roger. Optimizing neural networks with kronecker-factored approximate curvature. In *International conference on machine learning*, pp. 2408–2417, 2015.

Merity, Stephen, Keskar, Nitish Shirish, and Socher, Richard. Regularizing and optimizing lstm language models. *arXiv preprint arXiv:1708.02182*, 2017.

Nesterov, Yurii. A method of solving a convex programming problem with convergence rate $o(1/k^2)$. volume 27, pp. 372–367, 1983.

Nesterov, Yurii. *Introductory lectures on convex optimization: A basic course*, volume 87. Springer Science & Business Media, 2013.

O’donoghue, Brendan and Candes, Emmanuel. Adaptive restart for accelerated gradient schemes. *Foundations of computational mathematics*, 15(3):715–732, 2015.

Paszke, Adam, Gross, Sam, Chintala, Soumith, Chanan, Gregory, Yang, Edward, DeVito, Zachary, Lin, Zeming, Desmaison, Alban, Antiga, Luca, and Lerer, Adam. Automatic differentiation in pytorch. 2017.

Polyak, Boris T. Some methods of speeding up the convergence of iteration methods. *USSR Computational Mathematics and Mathematical Physics*, 4(5):1–17, 1964.

Polyak, Boris T and Juditsky, Anatoli B. Acceleration of stochastic approximation by averaging. *SIAM Journal on Control and Optimization*, 30(4):838–855, 1992.

Srinivasan, Vishwak, Sankar, Adepu Ravi, and Balasubramanian, Vineeth N. Adine: an adaptive momentum method for stochastic gradient descent. In *Proceedings of the ACM India Joint International Conference on Data Science and Management of Data*, pp. 249–256. ACM, 2018.

Sutskever, Ilya, Martens, James, Dahl, George, and Hinton, Geoffrey. On the importance of initialization and momentum in deep learning. In *International conference on machine learning*, pp. 1139–1147, 2013.

Tieleman, Tijmen and Hinton, Geoffrey. Lecture 6.5-
rmsprop: Divide the gradient by a running average of
its recent magnitude. *COURSERA: Neural networks for
machine learning*, 4(2):26–31, 2012.

Werbos, Paul J. Backpropagation through time: what it
does and how to do it. *Proceedings of the IEEE*, 78(10):
1550–1560, 1990.

Wilson, Ashia C, Roelofs, Rebecca, Stern, Mitchell, Srebro,
Nati, and Recht, Benjamin. The marginal value of adap-
tive gradient methods in machine learning. In *Advances in
Neural Information Processing Systems*, pp. 4151–4161,
2017.

Zeiler, Matthew D. Adadelta: an adaptive learning rate
method. *arXiv preprint arXiv:1212.5701*, 2012.

Zinkevich, Martin. Online convex programming and gen-
eralized infinitesimal gradient ascent. In *Proceedings of
the 20th International Conference on Machine Learning
(ICML-03)*, pp. 928–936, 2003.

Appendices

A. Nesterov Equivalence

We showed that when β is sufficiently close to 1 the Nesterov momentum update is approximately equivalent to the AggMo update in the special case where $\beta = [0, \beta]$. In this section we demonstrate this equivalence on two toy problems. In each of the figures included here we take $\beta = 0.999$.

We first consider a 2D quadratic function, $f(\mathbf{x}) = \mathbf{x}^T A \mathbf{x}$, where A has eigenvalues 1.0 and 0.001. We set the learning rate of AggMo to 2γ and Nesterov momentum to γ . Each optimizer is initialized at the same position. Figure 6 shows the optimization trajectories of both algorithms. In this setting the paths are indistinguishable.

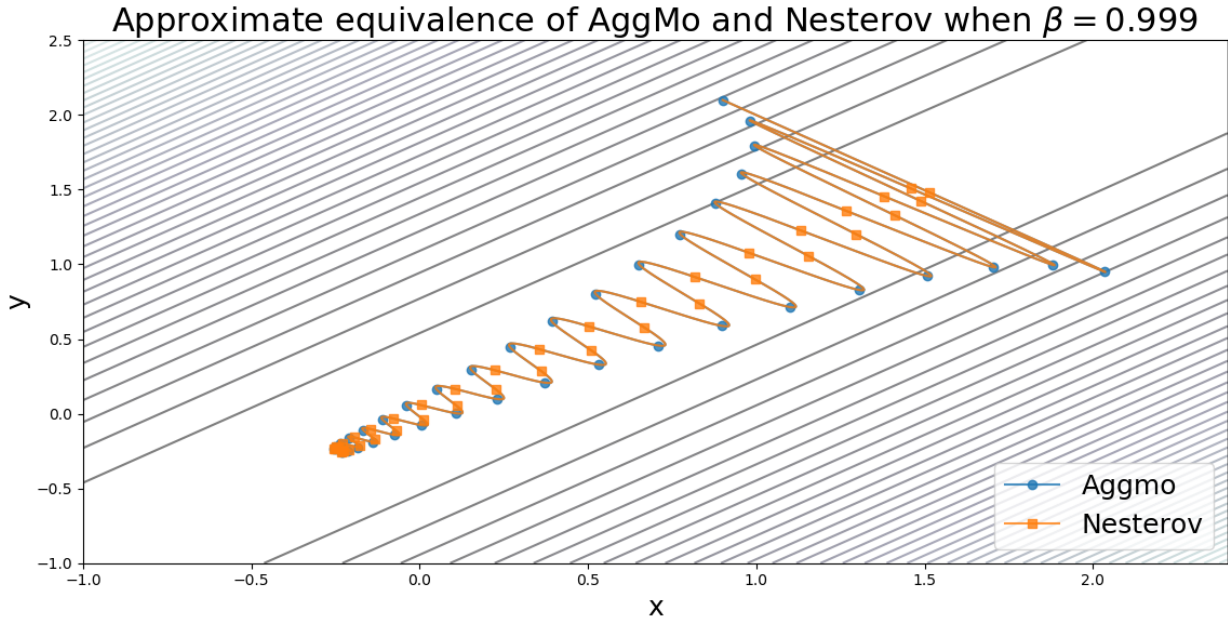


Figure 6. Approximate equivalence of Nesterov and AggMo when $\beta = 0.999$. The optimization plots for $f(x) = \mathbf{x}^T A \mathbf{x}$ are visibly identical (circles correspond to AggMo and squares to Nesterov - the markers are offset for readability).

We now optimize the Rosenbrock function, given by,

$$f(x, y) = (y - x^2)^2 + 100(x - 1)^2$$

This function has a global minimum at $(x, y) = 1$. Once again the optimizers are initialized at the same point and with the appropriately scaled learning rates. Figure 7 shows the optimization trajectories of both algorithms. In this case we see that the updates are initially indistinguishable but begin to differ as the algorithms approach the origin.

B. Convergence Proof

Here we present the proof of Theorem 4.1. We introduce some simplifying notation used in Duchi et al. (2011). We write $g_t = \nabla f(\theta_t)$, with $g_{t,i}$ denoting the i^{th} element of the vector g_t . We further write $g_{1:t,i} \in \mathbb{R}^t$ for the i^{th} dimension of gradients up to iteration t .

We begin with the following lemma,

Lemma 1. *Assume g_t is bounded, then the following holds,*

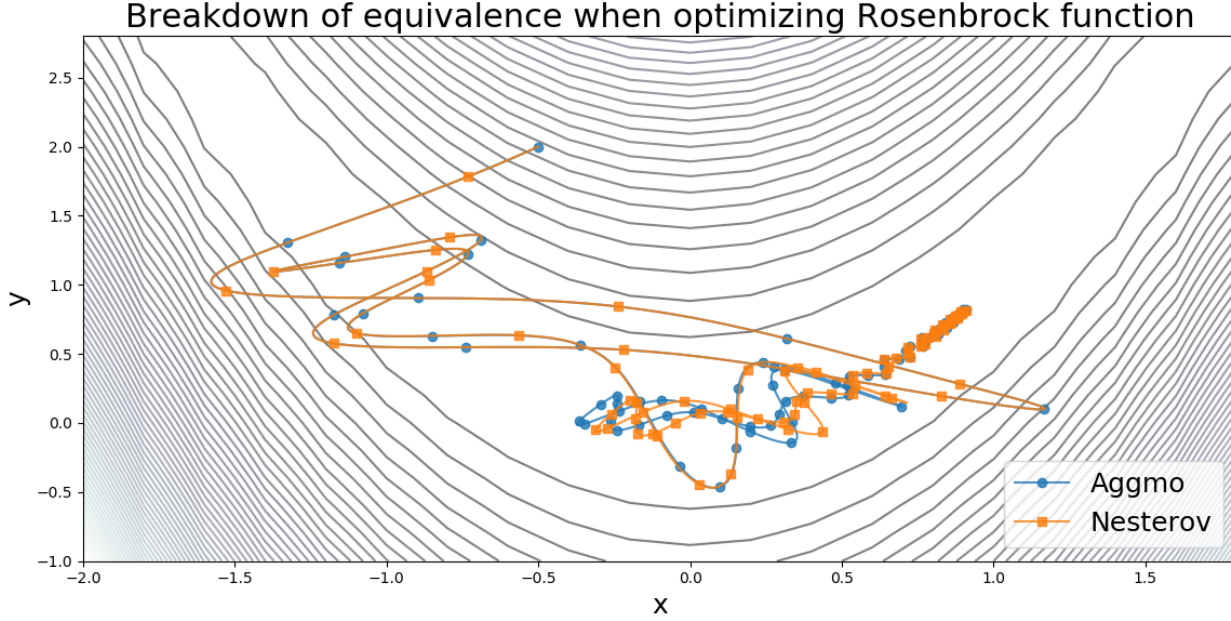


Figure 7. Approximate equivalence of Nesterov and AggMo when $\beta = 0.999$. The optimization trajectories are initially visibly identical but begin to differ slightly after more iterations.

$$\sum_{t=1}^T \sum_{i=1}^K \frac{\mathbf{v}_{t,i}^2}{\sqrt{t}} \leq \|g_{1:T,i}\|_4^2 \sqrt{1 + \log(T)} \sum_{i=1}^K \frac{1}{(1 - \beta^{(i)})^2}$$

Proof We begin by expanding the last term in the sum using the update equations,

$$\begin{aligned} \sum_{t=1}^T \sum_{i=1}^K \frac{\mathbf{v}_{t,i}^2}{\sqrt{t}} &= \sum_{t=1}^{T-1} \sum_{i=1}^K \frac{\mathbf{v}_{t,i}^2}{\sqrt{t}} + \frac{1}{\sqrt{T}} \sum_{i=1}^K \left(\sum_{j=1}^T (\beta_t^{(i)})^{T-j} g_j \right)^2 \\ &\leq \sum_{t=1}^{T-1} \sum_{i=1}^K \frac{\mathbf{v}_{t,i}^2}{\sqrt{t}} + \frac{1}{\sqrt{T}} \sum_{i=1}^K \left(\sum_{j=1}^T (\beta^{(i)})^{T-j} \right) \left(\sum_{j=1}^T (\beta^{(i)})^{T-j} g_j^2 \right) \\ &\leq \sum_{t=1}^{T-1} \sum_{i=1}^K \frac{\mathbf{v}_{t,i}^2}{\sqrt{t}} + \frac{1}{\sqrt{T}} \sum_{i=1}^K \frac{1}{1 - \beta^{(i)}} \left(\sum_{j=1}^T (\beta^{(i)})^{T-j} g_j^2 \right) \end{aligned}$$

The first inequality is obtained via Cauchy-Schwarz and by noting that $\beta_t^{(i)} \leq \beta$ for all t . The second inequality follows directly from the fact that $\sum_{j=1}^T (\beta^{(i)})^{T-j} < 1/(1 - \beta^{(i)})$. We can apply this upper bound to each term of the sum over t ,

$$\begin{aligned}
 \sum_{t=1}^T \sum_{i=1}^K \frac{\mathbf{v}_{t,i}^2}{\sqrt{t}} &\leq \sum_{t=1}^T \sum_{i=1}^K \frac{1}{\sqrt{t}(1-\beta^{(i)})} \sum_{j=1}^t (\beta^{(i)})^{t-j} g_j^2 \\
 &= \sum_{i=1}^K \frac{1}{1-\beta^{(i)}} \sum_{t=1}^T \frac{1}{\sqrt{t}} \sum_{j=1}^t (\beta^{(i)})^{t-j} g_j^2 \\
 &= \sum_{i=1}^K \frac{1}{1-\beta^{(i)}} \sum_{t=1}^T g_t^2 \sum_{j=1}^t \frac{(\beta^{(i)})^{j-t}}{\sqrt{j}} \\
 &\leq \sum_{i=1}^K \frac{1}{1-\beta^{(i)}} \sum_{t=1}^T g_t^2 \sum_{j=1}^t \frac{(\beta^{(i)})^{j-t}}{\sqrt{t}} \\
 &\leq \sum_{i=1}^K \frac{1}{(1-\beta^{(i)})^2} \sum_{t=1}^T g_t^2 \frac{1}{\sqrt{t}} \\
 &\leq \sum_{i=1}^K \frac{1}{(1-\beta^{(i)})^2} \|g_{1:T,i}\|_4^2 \sqrt{\sum_{t=1}^T \frac{1}{t}} \\
 &\leq \|g_{1:T,i}\|_4^2 \sqrt{1 + \log(T)} \sum_{i=1}^K \frac{1}{(1-\beta^{(i)})^2}
 \end{aligned}$$

Under equality we swap the order of sums and collect terms under g_t . The third inequality follows from $\sum_{j=1}^t (\beta^{(i)})^{j-t} < 1/(1-\beta)$. The fourth inequality is an application of Cauchy-Schwarz. The final inequality is from the harmonic sum bound: $\sum_{t=1}^T 1/t \leq 1 + \log(T)$. This completes the proof.

Proof of Theorem 1 From the update equations we may write,

$$\begin{aligned}
 \boldsymbol{\theta}_{t+1} &= \boldsymbol{\theta}_t + \frac{\gamma_t}{K} \sum_{i=1}^K \mathbf{v}_t^{(i)} \\
 &= \boldsymbol{\theta}_t + \frac{\gamma_t}{K} \sum_{i=1}^K (\beta_t^{(i)} \mathbf{v}_{t-1}^{(i)} - g_t)
 \end{aligned}$$

We now shift focus to only the j^{th} dimension. We subtract $\boldsymbol{\theta}_j^*$ from both sides and square,

$$(\boldsymbol{\theta}_{t+1,j} - \boldsymbol{\theta}_j^*)^2 = (\boldsymbol{\theta}_{t,j} - \boldsymbol{\theta}_j^*)^2 + 2 \frac{\gamma_t}{K} (\boldsymbol{\theta}_{t,j} - \boldsymbol{\theta}_j^*) \sum_{i=1}^K (\beta_t^{(i)} \mathbf{v}_{t-1,j}^{(i)} - g_{t,j}) + \frac{\gamma_t^2}{K^2} \left(\sum_{i=1}^K \mathbf{v}_{t,j}^{(i)} \right)^2$$

We can rearrange this expression and bound as follows,

$$\begin{aligned}
 g_{t,j}(\boldsymbol{\theta}_{t,j} - \boldsymbol{\theta}_j^*) &= \frac{K}{2\gamma_t} [(\boldsymbol{\theta}_{t,j} - \boldsymbol{\theta}_j^*)^2 - (\boldsymbol{\theta}_{t+1,j} - \boldsymbol{\theta}_j^*)^2] + (\boldsymbol{\theta}_{t,j} - \boldsymbol{\theta}_j^*) \sum_{i=1}^K (\beta_t^{(i)} \mathbf{v}_{t-1,j}^{(i)}) + \frac{\gamma_t}{2K} (\sum_{i=1}^K \mathbf{v}_{t,j}^{(i)})^2 \\
 &= \frac{K}{2\gamma_t} [(\boldsymbol{\theta}_{t,j} - \boldsymbol{\theta}_j^*)^2 - (\boldsymbol{\theta}_{t+1,j} - \boldsymbol{\theta}_j^*)^2] + \sum_{i=1}^K (\boldsymbol{\theta}_{t,j} - \boldsymbol{\theta}_j^*) (\beta_t^{(i)} \mathbf{v}_{t-1,j}^{(i)}) + \frac{\gamma_t}{2K} (\sum_{i=1}^K \mathbf{v}_{t,j}^{(i)})^2 \\
 &= \frac{K}{2\gamma_t} [(\boldsymbol{\theta}_{t,j} - \boldsymbol{\theta}_j^*)^2 - (\boldsymbol{\theta}_{t+1,j} - \boldsymbol{\theta}_j^*)^2] + \sum_{i=1}^K \frac{\sqrt{\beta_t^{(i)}}}{\sqrt{\gamma_{t-1}}} (\boldsymbol{\theta}_{t,j} - \boldsymbol{\theta}_j^*) \sqrt{\gamma_{t-1} \beta_t^{(i)}} (\mathbf{v}_{t-1,j}^{(i)}) + \frac{\gamma_t}{2K} (\sum_{i=1}^K \mathbf{v}_{t,j}^{(i)})^2 \\
 &\leq \frac{K}{2\gamma_t} [(\boldsymbol{\theta}_{t,j} - \boldsymbol{\theta}_j^*)^2 - (\boldsymbol{\theta}_{t+1,j} - \boldsymbol{\theta}_j^*)^2] + \sum_{i=1}^K \frac{\beta_t^{(i)}}{2\gamma_{t-1}} (\boldsymbol{\theta}_{t,j} - \boldsymbol{\theta}_j^*)^2 \\
 &\quad + \sum_{i=1}^K \frac{\gamma_{t-1}}{2} \beta_t^{(i)} (\mathbf{v}_{t-1,j}^{(i)})^2 + \frac{\gamma_t}{2K} (\sum_{i=1}^K \mathbf{v}_{t,j}^{(i)})^2 \\
 &\leq \frac{K}{2\gamma_t} [(\boldsymbol{\theta}_{t,j} - \boldsymbol{\theta}_j^*)^2 - (\boldsymbol{\theta}_{t+1,j} - \boldsymbol{\theta}_j^*)^2] + \sum_{i=1}^K \frac{\beta_t^{(i)}}{2\gamma_{t-1}} (\boldsymbol{\theta}_{t,j} - \boldsymbol{\theta}_j^*)^2 \\
 &\quad + \sum_{i=1}^K \frac{\gamma_{t-1}}{2} \beta_t^{(i)} (\mathbf{v}_{t-1,j}^{(i)})^2 + \frac{\gamma_t}{2} \sum_{i=1}^K (\mathbf{v}_{t,j}^{(i)})^2
 \end{aligned}$$

The first inequality is an application of Young's inequality. For the second inequality we use the sum-of-squares inequality. We now make use of convexity, and take the sum over dimensions and time,

$$\begin{aligned}
 \sum_{t=1}^T f_t(\boldsymbol{\theta}_t) - f_t(\boldsymbol{\theta}^*) &\leq \sum_{t=1}^T \sum_{j=1}^d g_{t,j}(\boldsymbol{\theta}_{t,j} - \boldsymbol{\theta}_j^*) \\
 &\leq \sum_{t=1}^T \sum_{j=1}^d \frac{K}{2\gamma_t} [(\boldsymbol{\theta}_{t,j} - \boldsymbol{\theta}_j^*)^2 - (\boldsymbol{\theta}_{t+1,j} - \boldsymbol{\theta}_j^*)^2] + \sum_{i=1}^K \frac{\beta_t^{(i)}}{2\gamma_{t-1}} (\boldsymbol{\theta}_{t,j} - \boldsymbol{\theta}_j^*)^2 \\
 &\quad + \sum_{i=1}^K \frac{\gamma_{t-1}}{2} \beta_t^{(i)} (\mathbf{v}_{t-1,j}^{(i)})^2 + \frac{\gamma_t}{2} \sum_{i=1}^K (\mathbf{v}_{t,j}^{(i)})^2 \\
 &\leq \sum_{j=1}^d \frac{K}{2\gamma_1} (\boldsymbol{\theta}_{1,j} - \boldsymbol{\theta}_j^*)^2 + \frac{K}{2} \sum_{j=1}^d \sum_{t=1}^T (\boldsymbol{\theta}_{t,j} - \boldsymbol{\theta}_j^*)^2 \left(\frac{1}{\gamma_t} - \frac{1}{\gamma_{t-1}} \right) \\
 &\quad + \sqrt{1 + \log(T)} \sum_{j=1}^d \|g_{1:T,j}\|_4^2 \sum_{i=1}^K \frac{1 + \beta^{(i)}}{(1 - \beta^{(i)})^2} \\
 &\quad + \sum_{i=1}^K \sum_{j=1}^d \sum_{t=1}^T \frac{\beta_t^{(i)}}{2\gamma_{t-1}} (\boldsymbol{\theta}_{t,j} - \boldsymbol{\theta}_j^*)^2
 \end{aligned}$$

We now make use of the bounding assumptions, $\|\boldsymbol{\theta}_m - \boldsymbol{\theta}_n\|_2 \leq D$ and $\|\boldsymbol{\theta}_m - \boldsymbol{\theta}_n\|_\infty \leq D_\infty$,

$$R(T) \leq \frac{KD_\infty^2 \sqrt{T}}{\gamma} + \sqrt{1 + \log(T)} \sum_{j=1}^d \|g_{1:T,j}\|_4^2 \sum_{i=1}^K \frac{1 + \beta^{(i)}}{(1 - \beta^{(i)})^2} + \frac{D^2}{2\gamma} \sum_{i=1}^K \sum_{t=1}^T \beta^{(i)} \lambda^{t-1} \sqrt{t}$$

The first two terms are collapsed using a telescoping sum. Using $\sum_t \lambda^{t-1} \sqrt{t} \leq 1/(1-\lambda)^2$, we achieve the following bound,

$$R(T) \leq \frac{KD_\infty^2 \sqrt{T}}{\gamma} + \sqrt{1 + \log(T)} \sum_{j=1}^d \|g_{1:T,j}\|_4^2 \sum_{i=1}^K \frac{1 + \beta^{(i)}}{(1 - \beta^{(i)})^2} + \frac{D^2}{2\gamma(1-\lambda)^2} \sum_{i=1}^K \beta^{(i)}$$

C. Experiments

All of our experiments are conducted using the pytorch library (Paszke et al., 2017). In each experiment we make use of early stopping to determine the run with the best validation performance.

C.1. Autoencoders

For the autoencoders we train fully connected networks with encoders using the following architecture: 784-1000-500-250-30. The decoder reverses this architecture. We use relu activations throughout the network. We train for a total of 1000 epochs using a multiplicative learning rate decay of 0.1 at 200, 400, and 800 epochs. We train using batch sizes of 200.

For these experiments the training set consists of 90% of the training data with the remaining 10% being used for validation. Details of the hyperparameter search are contained within the main paper body.

C.2. Classification

For each of the classification tasks we train for a total of 500 epochs using batchsizes of 128. We make use of a multiplicative learning rate decay of 0.1 at 150 and 250 epochs. For each of these experiments we use 80% of the training data for training and use the remaining 20% as validation. Details of the hyperparameter search for each experiment is contained within the main paper body.

CNN-5 The CNN-5 model uses relu activations throughout and 2x2 max pooling with stride 2. The first convolutional layer uses an 11x11 kernel with a stride of 4. This is followed by a max pooling layer. There is then a 5x5 convolutional kernel followed by max pooling. The network then uses three 3x3 convolutional layers and a final max pooling layer before feeding into a fully connected output layer. We do not use any regularization when training this model.

ResNet-34 We use the ResNet-34 architecture on both CIFAR-10 and CIFAR-100. We make use of a weight decay of 0.0005 and use batch normalization. We introduce data augmentation by using random crops with a padding of 4 and use random horizontal flips with probability 0.5.

C.3. LSTM Language Modelling

We train LSTMs with 3-layers containing 1150 hidden units per layer, and a 400 embedding size. Within the network we use dropout on the layers with probability 0.4. The hidden layers use dropout with probability 0.3 and the input embedding layers use dropout with probability 0.65 while the embedding layer itself uses dropout with probability 0.1. We also apply the weight drop method proposed in Merity et al. (2017) with probability 0.5. L2 regularization is applied on the RNN activations with a scaling of 2.0, we also use temporal activation regularization (slowness regularization) with scaling 1.0. Finally, all weights receive a weight decay of 1.2e-6.

We train the model using variable sequence lengths and batch sizes of 80. We measure the validation loss during training and decrease the learning rate if the validation loss has not decreased for 15 epochs. We found that a learning rate decay of 0.5 worked best for all optimizers except for SGD which achieved best performance with a fixed learning rate.

D. Additional Results

In this section we display some of the experimental results which we are unable to fit in the main paper.

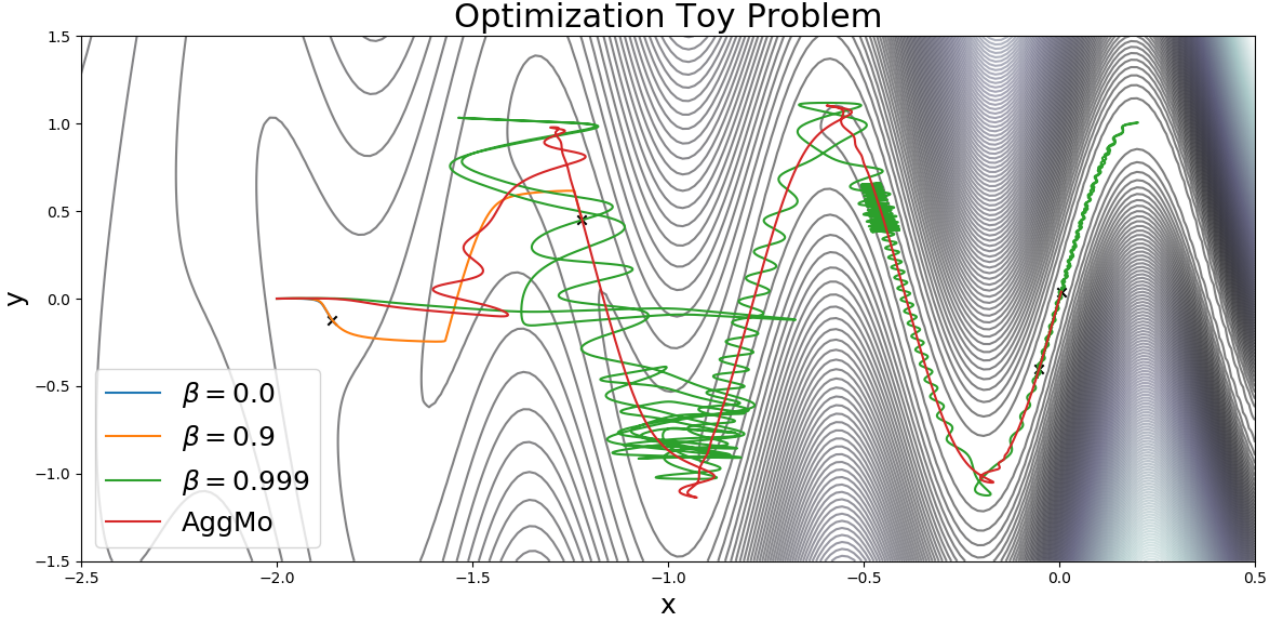


Figure 8. Comparison of classical momentum and aggregated momentum on toy problem (8) with $a = 8, b = 10$. In each case the optimizer is initialized at $(x, y) = (-2, 0)$

D.1. Toy Problem

To better understand how AggMo is able to help in non-convex settings we explore its effectiveness on a simple non-convex toy problem. The function we aim to optimize is defined as follows,

$$f(x, y) = \log(e^x + e^{-x}) + b \log \left(e^{e^x(y - \sin(ax))} + e^{-e^x(y - \sin(ax))} \right) \quad (8)$$

where a and b are constants which may be varied. We choose this function because it features flat regions and a series of non-convex funnels with varied curvature. The optimizer must traverse the flat regions quickly whilst remaining stable within the funnels. This function has an optimal value at $(x, y) = (0, 0)$.

Figure 8 compares the performance of classical momentum and aggregated momentum when optimizing Equation 8 with $a = 8, b = 10$. We see that GD with $\beta = 0$ and $\beta = 0.9$ are unable to leave the flat region around $x < -1$. For GD with $\beta = 0.999$ the optimizer enters the funnels but frequently becomes unstable with oscillations and finally overshoots the optimum. Compared to GD, AggMo is able to quickly traverse both the flat region and the funnels while remaining stable. AggMo also successfully slows down quickly once reaching the optimum.

E. Beta-Averaged Momentum

In this section we present a continuous analog of AggMo which provides additional insight into its effectiveness.

The AggMo update rule features the average of several velocities with some chosen damping coefficients, β . A natural extension to this formulation would be the expectation over an *iid* set of damping coefficients, $b \sim p(b)$. Explicitly, we write this update rule as,

$$\begin{aligned}\mathbf{v}_t &= b\mathbf{v}_{t-1} - \nabla_{\theta}f(\boldsymbol{\theta}_{t-1}) \\ \mathbf{x}_t &= \mathbf{x}_{t-1} + \gamma \mathbb{E}[\mathbf{v}_t]\end{aligned}\tag{9}$$

We may now consider the velocity as a stochastic process and the position is updated according to the average state at time t . We can link this back to aggregated momentum in the following way. If we sampled $b^{(i)}$ from $p(b)$ for $i = 1 : M$ then the procedure described by Equation 3 is approximating Equation 9 via Monte Carlo Integration.

Although this seems like a reasonable idea, it is not obvious whether we can compute this expectation in closed form. It turns out that with some conditions on $p(b)$ we can - namely that we have closed form solutions for the raw moments of $b \sim p(b)$. We can understand this update rule by expanding \mathbf{v}_t recursively,

$$\begin{aligned}\mathbf{v}_t &= b\mathbf{v}_{t-1} - \nabla_{\theta}f(\boldsymbol{\theta}_{t-1}) \\ &= b(b\mathbf{v}_{t-2} - \nabla_{\theta}f(\boldsymbol{\theta}_{t-2})) - \nabla_{\theta}f(\boldsymbol{\theta}_{t-1}) \\ &= b^t\mathbf{v}_0 - \sum_{i=1}^t b^{i-1}\nabla_{\theta}f(\boldsymbol{\theta}_{t-i}) \\ &= -\sum_{i=1}^t b^{i-1}\nabla_{\theta}f(\boldsymbol{\theta}_{t-i}) = -\sum_{i=0}^{t-1} b^{t-i-1}\nabla_{\theta}f(\boldsymbol{\theta}_i)\end{aligned}\tag{10}$$

Thus we can write the update rule for \mathbf{x}_t as,

$$\mathbf{x}_t = \mathbf{x}_{t-1} - \gamma \sum_{i=1}^t \mathbb{E}[b^{i-1}]\nabla_{\theta}f(\boldsymbol{\theta}_{t-i})\tag{11}$$

Thus to compute the update rule we must compute the raw moments of b . If we take $b \sim Beta(\alpha, \beta)$ (*note that this β is different to the damping coefficient previously using this notation*) then these raw moments have a closed form:

$$\mathbb{E}[b^k] = \prod_{r=0}^{k-1} \frac{\alpha + r}{\alpha + \beta + r}\tag{12}$$

This provides a closed form solution to compute \mathbf{x}_t given \mathbf{x}_{t-1} and the history of all previous gradients. We refer to this update scheme as *Beta-Averaged Momentum*. Unfortunately, each update requires the history of all previous gradients to be computed. We may find some reasonable approximation to the update rule. For example, we could keep only the T most recently computed gradients.

Figure 9 shows the optimization of 1D quadratics using Beta-Averaged Momentum. The trajectories are similar to those achieved using the original AggMo formulation.

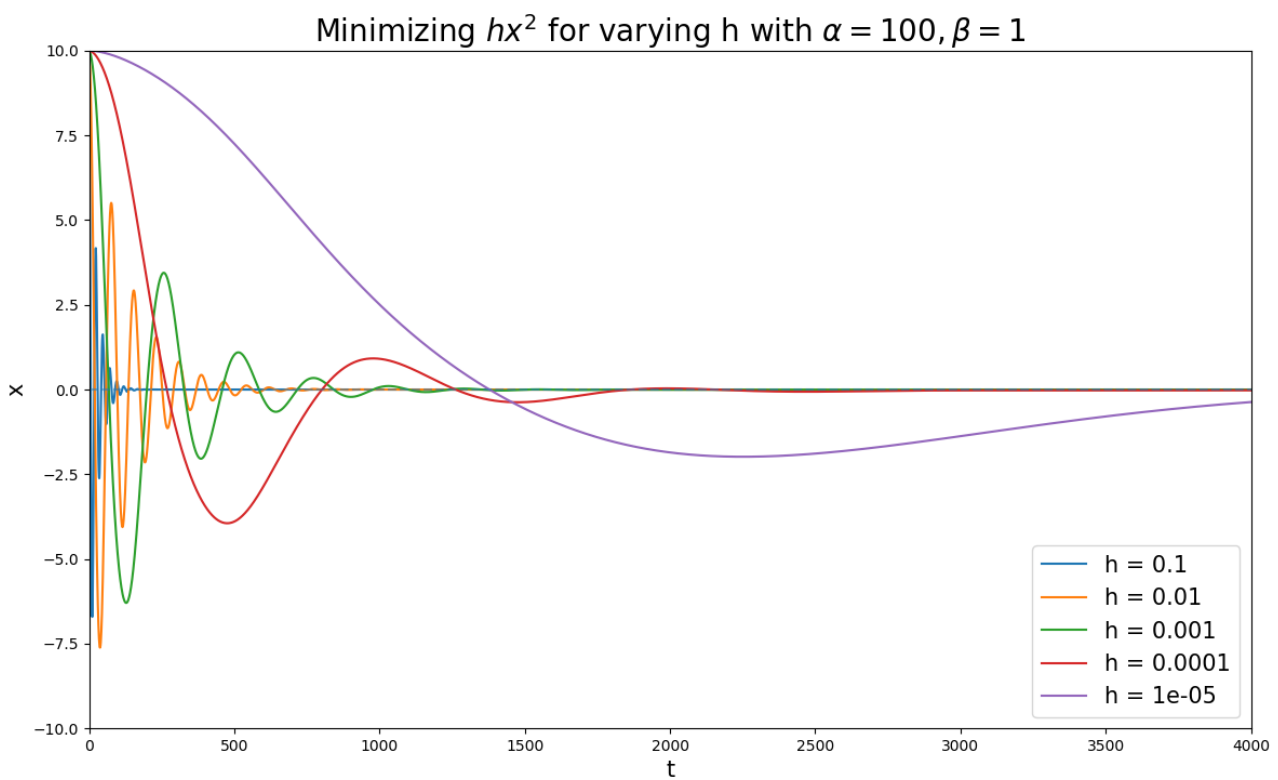


Figure 9. Beta-Averaged GD with a Beta prior on momentum ($\alpha = 100, \beta = 1$).